Transactions of the Nigerian Association of Mathematical Physics
Volume 13, (October – December, 2020 Issue), **pp61 –68**

FIRST PRINCIPLE AND ANALYTICAL CALCULATIONS OF THE LATTICE DYNAMICS OF MO AND TA

[1]Okocha O.G. and [2]Osuhor O.P.

[1]Science Laboratory Technology, Federal Polytechnic, Auchi, Edo State.
[2]Department of Physics, University of Benin, Benin City.

Abstract

The phonon dispersion curves of Mo and Ta have been calculated from analytical (IFCs technique using Born – von Kármán model) with different numbers of interacting nearest-neighbours (NN) and computational approach (first principle using density functional theory) with the exchange correlation functionals. The different branches of the phonon band structure follow from the Eigen values after diagonalizing the dynamical matrix. The phonon frequencies in the first Brillouin zone were calculated along the directions of high symmetry, $\Gamma \rightarrow H$, $H \rightarrow P$, $P \rightarrow \Gamma$ and $\Gamma \rightarrow N$. Obtain also are the thermodynamic properties from analytical and first principle. It is observed that the phonon dispersion curve of Mo from first principle calculation is in better agreement with experiment compared to the IFCs calculation, whereas, the phonon dispersion curve of Ta from IFCs is in better agreement with experiment compared to the first principle calculation.

Keywords: Bcc Metals, Phonon, Interatomic Force Constants, Dynamical Matrix, Born – von Kármán.

1.0 INTRODUCTION

It is a fact that phonons play a vital role in several important phenomena in modern and classical solid state physics. Thus, a vast number of physical properties hinge on the behaviour of their lattice dynamics and it follows that the force model, if given a good fit to the dispersion foretell brilliantly all other properties of the lattice dynamics [1, 2]. Currently, it is feasible to calculate specific properties of specific materials applying first principle techniques in quantum-mechanics in computational material science and condensed-matter theoretical physics with the chemical composition of the materials as its only input information. Accordingly, for a particular case of the properties of lattice dynamics, a considerable number of first principle calculations on the basis of the theory of linear response of the vibrations of lattice is feasible now by the success of density functional theory (DFT) [3, 4] coupled with the occurrence of density-functional perturbation theory (DFPT) [5, 6]. The DFPT is a technique used in employing the DFT in the heart of general theoretical architecture. Thus, making it feasible to produce accurately the dispersion curves of phonon on a smooth grating of wave vectors which encompass the whole Brillouin zone (BZ).

The first principle prediction of the dispersion curves of phonon of noble and transition metals have encountered challenges that still lack adequate solution from the generally used exchange correlation functional "local density approximation (LDA) and the generalized gradient approximation (GGA)" [4, 8, 9]. To improve on the first principle calculation results, the density functional theory was applied [10] with variation in the exchange and correlation functional being used, the dispersion curves can in some cases underestimate or overestimate when compared to experimental results. This brings us to the question, if the first principle (QUANTUM ESPRESSO) calculation [11, 12] is still having these challenges, is it also possible for us to tackle the phonon dispersion problem using the interatomic force constant technique as implemented in the Born-von Kármán model? The challenge here is to determine and improve on existing techniques employed to determine the lattice dynamics of Mo and Ta using analytical approach (interatomic force constants – IFCs) and computational approach (first principle or ab-initio – QUANTUM ESPRESSO) and compare with experiment. Also calculated are their thermodynamic properties.

2.0 THEORETICAL FORMALISM

2.1 ANALYTICAL (IFCs) PROCEDURE

The Born-von Kármán theory was applied by assigning a force-constant matrix to each of the nearest neighbours of the

Correspondence Author: Okocha O.G., Email: obitex5555@gmail.com, Tel: +2348055587223

atom considered, constructing the dynamical matrix from the individual force-constant matrices, and then solving the dynamical matrix for the phonon energies and the associated phonon polarizations.

CONSTRUCTION OF THE DYNAMICAL MATRIX

The phonon frequencies are given by the solution of the secular determinant

$$\left|D_{\mathrm{ij}}(\vec{q}) - m\omega^2 I\right| = 0 \tag{1}$$

Where m is the mass of the ion, ω is the phonon frequency, $D_{\mathrm{ij}}(\vec{q})$ is the dynamical matrix elements and I is a 3×3 unit matrix. The elements of the dynamical matrix are a matrix as shown below

$$D_{\mathrm{ij}} = \begin{pmatrix} D_{\mathrm{xx}}(\vec{q}) & D_{\mathrm{xy}}(\vec{q}) & D_{\mathrm{xz}}(\vec{q}) \\ D_{\mathrm{yx}}(\vec{q}) & D_{\mathrm{yy}}(\vec{q}) & D_{\mathrm{yz}}(\vec{q}) \\ D_{\mathrm{zx}}(\vec{q}) & D_{\mathrm{zy}}(\vec{q}) & D_{\mathrm{zz}}(\vec{q}) \end{pmatrix} \tag{2}$$

Once the force constant matrices have been determined the elements of the dynamical matrix are evaluated. This gives for the diagonal matrix elements of the first nearest to eighth nearest neighbours dynamical matrix as:

$$\begin{aligned} D_{xx}(\vec{q}) = \frac{1}{M}\{ & 8\alpha_1 + 2\alpha_2 + 4\beta_2 + 8\alpha_3 + 4\beta_3 + 8\alpha_4 + 16\beta_4 + 8\alpha_5 + 2\alpha_6 + 4\beta_6 + 8\alpha_7 + 16\beta_7 \\ & + 8\alpha_8 + 8\beta_8 + 8\gamma_8 + 8\alpha_9 + 16\beta_9 + 8\alpha_{10} - 8\alpha_1 \cos\left(\frac{aq_x}{2}\right)\cos\left(\frac{aq_y}{2}\right)\cos\left(\frac{aq_z}{2}\right) \\ & - 2\alpha_2 \cos(aq_x) - 2\beta_2 \cos(aq_y) - 2\beta_2 \cos(aq_z) - 4\alpha_3 \cos(aq_x)\cos(aq_y) \\ & - 4\alpha_3 \cos(aq_x)\cos(aq_z) - 4\beta_3 \cos(aq_x)\cos(aq_y) - 8\alpha_4 \cos\left(\frac{3aq_x}{2}\right)\cos\left(\frac{aq_y}{2}\right)\cos\left(\frac{aq_z}{2}\right) \\ & - 8\beta_4 \cos\left(\frac{aq_x}{2}\right)\cos\left(\frac{3aq_y}{2}\right)\cos\left(\frac{aq_z}{2}\right) - 8\beta_4 \cos\left(\frac{aq_x}{2}\right)\cos\left(\frac{aq_y}{2}\right)\cos\left(\frac{3aq_z}{2}\right) \\ & - 8\alpha_5 \cos(aq_x)\cos(aq_y)\cos(aq_z) - 2\alpha_6 \cos(2aq_x) - 2\beta_6 \cos(2aq_y) - 2\beta_6 \cos(2aq_z) \\ & - 8\alpha_7 \cos\left(\frac{aq_x}{2}\right)\cos\left(\frac{3aq_y}{2}\right)\cos\left(\frac{3aq_z}{2}\right) - 8\beta_7 \cos\left(\frac{3aq_x}{2}\right)\cos\left(\frac{3aq_y}{2}\right)\cos\left(\frac{aq_z}{2}\right) \\ & - 8\beta_7 \cos\left(\frac{3aq_x}{2}\right)\cos\left(\frac{3aq_y}{2}\right)\cos\left(\frac{aq_z}{2}\right) - 4\alpha_8 \cos(2aq_x)\cos(aq_y) - 4\alpha_8 \cos(2aq_x)\cos(aq_z) \\ & - 4\gamma_8 \cos(2aq_z)\cos(aq_y) - 4\gamma_8 \cos(2aq_y)\cos(aq_z) - 4\beta_8 \cos(aq_x)\cos(2aq_y) \\ & - 4\beta_8 \cos(aq_x)\cos(2aq_z) \} \end{aligned} \tag{3}$$

$$\begin{aligned} D_{yy}(\vec{q}) = \frac{1}{M}\{ & 8\alpha_1 + 2\alpha_2 + 4\beta_2 + 8\alpha_3 + 4\beta_3 + 8\alpha_4 + 16\beta_4 + 8\alpha_5 + 2\alpha_6 + 4\beta_6 + 8\alpha_7 + 16\beta_7 \\ & + 8\alpha_8 + 8\beta_8 + 8\gamma_8 + 8\alpha_9 + 16\beta_9 + 8\alpha_{10} - 8\alpha_1 \cos\left(\frac{aq_x}{2}\right)\cos\left(\frac{aq_y}{2}\right)\cos\left(\frac{aq_z}{2}\right) \\ & - 2\alpha_2 \cos(aq_y) - 2\beta_2 \cos(aq_x) - 2\beta_2 \cos(aq_z) - 4\alpha_3 \cos(aq_x)\cos(aq_y) \\ & - 4\alpha_3 \cos(aq_y)\cos(aq_z) - 4\beta_3 \cos(aq_x)\cos(aq_z) - 8\alpha_4 \cos\left(\frac{aq_x}{2}\right)\cos\left(\frac{3aq_y}{2}\right)\cos\left(\frac{aq_z}{2}\right) \\ & - 8\beta_4 \cos\left(\frac{3aq_x}{2}\right)\cos\left(\frac{aq_y}{2}\right)\cos\left(\frac{aq_z}{2}\right) - 8\beta_4 \cos\left(\frac{aq_x}{2}\right)\cos\left(\frac{aq_y}{2}\right)\cos\left(\frac{3aq_z}{2}\right) \\ & - 8\alpha_5 \cos(aq_x)\cos(aq_y)\cos(aq_z) - 2\alpha_6 \cos(2aq_x) - 2\beta_6 \cos(2aq_y) - 2\beta_6 \cos(2aq_z) \\ & - 8\alpha_7 \cos\left(\frac{3aq_x}{2}\right)\cos\left(\frac{aq_y}{2}\right)\cos\left(\frac{3aq_z}{2}\right) - 8\beta_7 \cos\left(\frac{aq_x}{2}\right)\cos\left(\frac{3aq_y}{2}\right)\cos\left(\frac{3aq_z}{2}\right) \\ & - 8\beta_7 \cos\left(\frac{3aq_x}{2}\right)\cos\left(\frac{3aq_y}{2}\right)\cos\left(\frac{aq_z}{2}\right) - 4\alpha_8 \cos(2aq_y)\cos(aq_z) - 4\alpha_8 \cos(aq_x)\cos(2aq_y) \\ & - 4\gamma_8 \cos(2aq_x)\cos(aq_z) - 4\gamma_8 \cos(2aq_x)\cos(aq_z) - 4\beta_8 \cos(2aq_x)\cos(aq_y) \\ & - 4\beta_8 \cos(aq_y)\cos(2aq_z) \} \end{aligned} \tag{4}$$

$$\begin{aligned} D_{zz}(\vec{q}) = \frac{1}{M}\{ & 8\alpha_1 + 2\alpha_2 + 4\beta_2 + 8\alpha_3 + 4\beta_3 + 8\alpha_4 + 16\beta_4 + 8\alpha_5 + 2\alpha_6 + 4\beta_6 + 8\alpha_7 + 16\beta_7 \\ & + 8\alpha_8 + 8\beta_8 + 8\gamma_8 + 8\alpha_9 + 16\beta_9 + 8\alpha_{10} - 8\alpha_1 \cos\left(\frac{aq_x}{2}\right)\cos\left(\frac{aq_y}{2}\right)\cos\left(\frac{aq_z}{2}\right) \\ & - 2\alpha_2 \cos(aq_z) - 2\beta_2 \cos(aq_x) - 2\beta_2 \cos(aq_y) - 4\alpha_3 \cos(aq_x)\cos(aq_z) \\ & - 4\alpha_3 \cos(aq_y)\cos(aq_z) - 4\beta_3 \cos(aq_x)\cos(aq_y) - 8\alpha_4 \cos\left(\frac{aq_x}{2}\right)\cos\left(\frac{aq_y}{2}\right)\cos\left(\frac{3aq_z}{2}\right) \\ & - 8\beta_4 \cos\left(\frac{3aq_x}{2}\right)\cos\left(\frac{aq_y}{2}\right)\cos\left(\frac{aq_z}{2}\right) - 8\beta_4 \cos\left(\frac{aq_x}{2}\right)\cos\left(\frac{3aq_y}{2}\right)\cos\left(\frac{aq_z}{2}\right) \\ & - 8\alpha_5 \cos(aq_x)\cos(aq_y)\cos(aq_z) - 2\alpha_6 \cos(2aq_z) - 2\beta_6 \cos(2aq_y) - 2\beta_6 \cos(2aq_x) \\ & - 8\alpha_7 \cos\left(\frac{3aq_x}{2}\right)\cos\left(\frac{3aq_y}{2}\right)\cos\left(\frac{aq_z}{2}\right) - 8\beta_7 \cos\left(\frac{aq_x}{2}\right)\cos\left(\frac{3aq_y}{2}\right)\cos\left(\frac{3aq_z}{2}\right) \\ & - 8\beta_7 \cos\left(\frac{3aq_x}{2}\right)\cos\left(\frac{aq_y}{2}\right)\cos\left(\frac{3aq_z}{2}\right) - 4\alpha_8 \cos(aq_x)\cos(2aq_z) - 4\alpha_8 \cos(aq_y)\cos(2aq_z) \\ & - 4\gamma_8 \cos(aq_x)\cos(2aq_y) - 4\gamma_8 \cos(2aq_x)\cos(aq_y) - 4\beta_8 \cos(2aq_x)\cos(aq_z) \\ & - 4\beta_8 \cos(2aq_y)\cos(aq_z) \} \end{aligned} \tag{5}$$

And the off - diagonal matrix elements of the first nearest to eighth nearest neighbour dynamical matrix as:

$$D_{xy} = \frac{1}{M}\left\{\begin{array}{l} 8\beta_1 \sin\left(\frac{aq_x}{2}\right)\sin\left(\frac{aq_y}{2}\right)\cos\left(\frac{aq_z}{2}\right) + 4\gamma_3 \sin\left(aq_x\right)\sin\left(aq_y\right) \\ + 8\gamma_4 \sin\left(\frac{3aq_x}{2}\right)\sin\left(\frac{aq_y}{2}\right)\cos\left(\frac{aq_z}{2}\right) + 8\gamma_4 \sin\left(\frac{aq_x}{2}\right)\sin\left(\frac{3aq_y}{2}\right)\cos\left(\frac{aq_z}{2}\right) \\ + 8\delta_4 \sin\left(\frac{aq_x}{2}\right)\sin\left(\frac{aq_y}{2}\right)\cos\left(\frac{3aq_z}{2}\right) + 8\beta_5 \sin\left(aq_x\right)\sin\left(aq_y\right)\cos\left(aq_z\right) \\ + 8\gamma_7 \sin\left(\frac{aq_x}{2}\right)\sin\left(\frac{3aq_y}{2}\right)\cos\left(\frac{3aq_z}{2}\right) + 8\gamma_7 \sin\left(\frac{3aq_x}{2}\right)\sin\left(\frac{aq_y}{2}\right)\cos\left(\frac{3aq_z}{2}\right) \\ + 8\delta_7 \sin\left(\frac{3aq_x}{2}\right)\sin\left(\frac{3aq_y}{2}\right)\cos\left(\frac{aq_z}{2}\right) + 4\delta_8 \sin\left(2aq_x\right)\sin\left(aq_y\right) \\ + 4\delta_8 \sin\left(aq_x\right)\sin\left(2aq_y\right) \end{array}\right\} \quad (6)$$

$$D_{xz} = \frac{1}{M}\left\{\begin{array}{l} 8\beta_1 \sin\left(\frac{aq_x}{2}\right)\sin\left(\frac{aq_z}{2}\right)\cos\left(\frac{aq_y}{2}\right) + 4\gamma_3 \sin\left(aq_x\right)\sin\left(aq_z\right) \\ + 8\gamma_4 \sin\left(\frac{3aq_x}{2}\right)\sin\left(\frac{aq_z}{2}\right)\cos\left(\frac{aq_y}{2}\right) + 8\gamma_4 \sin\left(\frac{aq_x}{2}\right)\sin\left(\frac{3aq_z}{2}\right)\cos\left(\frac{aq_y}{2}\right) \\ + 8\delta_4 \sin\left(\frac{aq_x}{2}\right)\sin\left(\frac{aq_z}{2}\right)\cos\left(\frac{3aq_y}{2}\right) + 8\beta_5 \sin\left(aq_x\right)\sin\left(aq_z\right)\cos\left(aq_y\right) \\ + 8\gamma_7 \sin\left(\frac{aq_x}{2}\right)\sin\left(\frac{3aq_z}{2}\right)\cos\left(\frac{3aq_y}{2}\right) + 8\gamma_7 \sin\left(\frac{3aq_x}{2}\right)\sin\left(\frac{aq_z}{2}\right)\cos\left(\frac{3aq_y}{2}\right) \\ + 8\delta_7 \sin\left(\frac{3aq_x}{2}\right)\sin\left(\frac{3aq_z}{2}\right)\cos\left(\frac{aq_y}{2}\right) + 4\delta_8 \sin\left(2aq_x\right)\sin\left(aq_z\right) \\ + 4\delta_8 \sin\left(aq_x\right)\sin\left(2aq_z\right) \end{array}\right\} \quad (7)$$

$$D_{yz} = \frac{1}{M}\left\{\begin{array}{l} 8\beta_1 \sin\left(\frac{aq_y}{2}\right)\sin\left(\frac{aq_z}{2}\right)\cos\left(\frac{aq_x}{2}\right) + 4\gamma_3 \sin\left(aq_y\right)\sin\left(aq_z\right) \\ + 8\gamma_4 \sin\left(\frac{3aq_y}{2}\right)\sin\left(\frac{aq_z}{2}\right)\cos\left(\frac{aq_x}{2}\right) + 8\gamma_4 \sin\left(\frac{aq_y}{2}\right)\sin\left(\frac{3aq_z}{2}\right)\cos\left(\frac{aq_x}{2}\right) \\ + 8\delta_4 \sin\left(\frac{aq_z}{2}\right)\sin\left(\frac{aq_y}{2}\right)\cos\left(\frac{3aq_x}{2}\right) + 8\beta_5 \sin\left(aq_y\right)\sin\left(aq_z\right)\cos\left(aq_z\right) \\ + 8\gamma_7 \sin\left(\frac{aq_y}{2}\right)\sin\left(\frac{3aq_z}{2}\right)\cos\left(\frac{3aq_x}{2}\right) + 8\gamma_7 \sin\left(\frac{3aq_y}{2}\right)\sin\left(\frac{aq_z}{2}\right)\cos\left(\frac{3aq_x}{2}\right) \\ + 8\delta_7 \sin\left(\frac{3aq_y}{2}\right)\sin\left(\frac{3aq_z}{2}\right)\cos\left(\frac{aq_x}{2}\right) + 4\delta_8 \sin\left(2aq_y\right)\sin\left(aq_z\right) \\ + 4\delta_8 \sin\left(aq_y\right)\sin\left(2aq_z\right) \end{array}\right\} \quad (8)$$

Where M denotes the mass of the element, and $D_{xy} = D_{yx}$, $D_{xz} = D_{zx}$ and $D_{yz} = D_{zy}$. The elements α_1, β_1, … are the nearest neighbour parameters in a least-squares fit to the data. The force constants were also of great value as a simple mathematical description of the phonon spectrum [13] used this property in their method of calculating the phonon distribution function.

2.2 COMPUTATIONAL PROCEDURE

The DFT calculations were performed using QUANTUM ESPRESSO (opEn Source Package for Research in Electronic Structure, Simulation, and Optimization) [11, 12]. This code uses plane-wave and pseudopotential method to describe the electron-ion interaction. In this research work, the local density approximation (LDA), Generalized Gradient Approximation (GGA) with exchange and correlation functional described by Perdew-Burke-Ernzerhof (PBE) [9]. Also, PAW and PW91 method were used to generate the pseudopotentials for the elements in this work.

The convergence of the total electronic energy as computed in plane-wave pseudopotential codes is determined by two key computational parameters, namely the number of basis functions (plane-wave cut-off) and the number of k-points (k-spacing). In this research work, the number of basis functions was determined by running series of self-consistent calculations for different values of kinetic energy cut-off (ecutwfc) starting from (10 to 70) Ry at an interval of 5Ry. The converged values were found to be between 25 to 65 Ry. Also, the k-points values are tin the range of 4 – 12 k-points meshes. All these assisted in determining accurately the electronic ground state properties of the systems studied in this work.

2.3 CALCULATION OF THE THERMODYNAMIC PROPERTIES OF BCC METALS

Thermodynamic functions of solids are determined by their vibrational degrees of freedom of their lattice [14]. Thus, for the calculation of these thermodynamic functions requires a complete knowledge of the vibrational spectrum, with adequate accuracy [15, 16, 17]. The phonon contributions to the thermodynamic properties which include Helmholtz free energy ΔF, the internal energy ΔE, the constant-volume specific heat C_v, and the entropy S are computed for these bcc metals studied in this work within the temperature range of 0 – 800K with the following expressions:

For the Helmholtz free energy

$$\Delta F = 3nNK_B T \ln\left\{\begin{array}{l} 2\sinh\left(\frac{\hbar\omega_1}{2K_BT}\right)g(\omega_1)\Delta\omega_1 + 2\sinh\left(\frac{\hbar\omega_2}{2K_BT}\right)g(\omega_2)\Delta\omega_2 \\ +\ldots+2\sinh\left(\frac{\hbar\omega_n}{2K_BT}\right)g(\omega_n)\Delta\omega_n \end{array}\right\} \quad (9)$$

For the internal energy we have

$$\Delta E = 3nN\frac{\hbar}{2}\ln\left\{\begin{array}{l} \omega\coth\left(\frac{\hbar\omega}{2K_BT}\right)g(\omega_1)\Delta\omega_1 + \omega\coth\left(\frac{\hbar\omega}{2K_BT}\right)g(\omega_2)\Delta\omega_2 \\ +\ldots+\omega\coth\left(\frac{\hbar\omega}{2K_BT}\right)g(\omega_n)\Delta\omega_n \end{array}\right\} \quad (10)$$

For the constant-volume specific heat we have

$$C_\upsilon = 3nNk_B\left\{\begin{array}{l} \left(\frac{\hbar\omega_1}{2K_BT}\right)^2\operatorname{csc}h^2\left(\frac{\hbar\omega_1}{2K_BT}\right)g(\omega_1)\Delta\omega_1 \\ +\left(\frac{\hbar\omega_2}{2K_BT}\right)^2\operatorname{csc}h^2\left(\frac{\hbar\omega_2}{2K_BT}\right)g(\omega_2)\Delta\omega_2+\ldots \\ +\left(\frac{\hbar\omega_n}{2K_BT}\right)^2\operatorname{csc}h^2\left(\frac{\hbar\omega_n}{2K_BT}\right)g(\omega_n)\Delta\omega_n \end{array}\right\} \quad (11)$$

Finally, for the entropy we have

$$S = 3nNk_B\left\{\begin{array}{l} \left[\frac{\hbar\omega_1}{2K_BT}\coth\frac{\hbar\omega_1}{2K_BT}-\ln\left(2\sinh\frac{\hbar\omega_1}{2K_BT}\right)\right]g(\omega)d\omega_1 \\ +\left[\frac{\hbar\omega_2}{2K_BT}\coth\frac{\hbar\omega_2}{2K_BT}-\ln\left(2\sinh\frac{\hbar\omega_2}{2K_BT}\right)\right]g(\omega)d\omega_2 \\ +\ldots+\left[\frac{\hbar\omega_n}{2K_BT}\coth\frac{\hbar\omega_n}{2K_BT}-\ln\left(2\sinh\frac{\hbar\omega_n}{2K_BT}\right)\right]g(\omega)d\omega_n \end{array}\right\} \quad (12)$$

Note: $\coth = \frac{1}{\tanh}$, $\operatorname{csc}h = \frac{1}{\sinh}$

Where K_B is the Boltzmann's constant, $\hbar$ is reduced Planck's constant

3.0 RESULTS AND DISCUSSION

3.1 Lattice dynamics

Fig. 1. shows the phonon dispersion curve of Molybdenum (Mo) from IFCs calculated up to fifth nearest neighbours implemented by Born – von Kármán model and matched with data from experiment. The data from experiment is presented in blue, green and red circles with the red solid line calculations from IFCs. Fig. 2. the black, red and blue solid curves are the dispersions calculated using the generalized gradient approximation (GGA-PBE), local density approximation (LDA)and PW91 respectively, with the experimental data in blue, green and red circles. Tables 1a and 1b show that the 5th nearest neighbours dispersions calculated with (MAE 0.1539THz, MARE 2.47%), did not improve the results when matched with experiment. Whereas, the DFT using GGA (PAW), PW91 and LDA gave (MAE 0.1200THz, MARE 1.92%), (MAE 0.0269THz, MARE 0.43%) and (MAE 0.1618THz, MARE 2.59%) respectively. In the first principle computations employing DFT, PW91 gave a better result when compared to GGA (PBE) and LDA. Also, the lattice constant given by PW91 is 1.23% above that of the experiment. This error was corrected by functionals of GGA (PAW) and LDA with only 0.72% above and 0.62% lower than experiment respectively. Fig. 3. shows the phonon dispersion curve of Tantalum (Ta) from IFCs calculated up to eighth nearest neighbours implemented into Born – von Kármán model and matched with data from experiment. The data from experiment is presented in blue, green and red circles with the red solid line calculations

from IFCs. Fig. 4. The experimental data is shown as blue, green and red circles, the black, red and blue solid curves are the dispersion calculated using GGA-PBE, PW91 and LDA respectively. In tables2a and 2b, IFCs calculations of the lattice dynamics of Tantalum (Ta) showed that the 8th nearest neighbours dispersions calculated with (MAE 0.0126THz), percentage error (MARE 0.31%) improve on the experimental results. Whereas, the density functional theory (DFT) using GGA (PBE), PW91 and LDA gave a larger MAE and MARE as (MAE 0.1008THz, MARE 2.66%), (MAE 1.1238THz, MARE 27.50%) and (MAE 1.6995THz, MARE 41.57%) respectively. In the first principle calculations using DFT, the GGA (PBE) functional gave a better result when compared to PW91 and LDA functionals. Also, the PW91 gave a better percentage error to the lattice constant by 0.50% slightly above experiment while GGA(PBE) and LDA overestimated and underestimated by 0.85% and 1.56% respectively

3.2 Thermodynamic properties

Figs.3 and 9. shows an increase in the internal energy as temperature increases and also at 0K it is above zero. Figs. 4 and 10. shows a decreases in the free energy within crease in temperature whereas in Figs. 5 and 11. shows an increase in the entropy with an increase in temperature. In Figs. 6 and 12. the heat capacity on the other hand shows a rapid increase with temperature and approaches the Dulong-Petit limit at high temperature and at low temperature the graph obeys the T^3 and at very low temperature the graph obeys the linear law as can be found in literature.

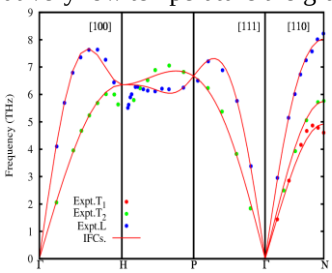

Fig 1: Molybdenum dispersion curves. The Red curves correspond to fifth nearest neighbours fit (IFCs). The experimental results [18]are shown by the symbols, and

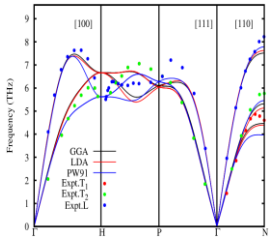

Fig 2: Molybdenum dispersion curves. GGA(PBE), the LDA and PW91 results from QUANTUM ESPRESSO calculations. The experimental results [18] are shown by the symbols, and

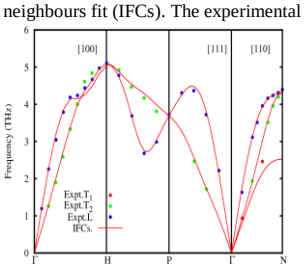

Fig 3: Tantalum dispersion curves. The Red curves correspond to eight nearest neighbours fit (IFCs). The experimental results from the inelastic neutron scattering data [19]are shown by the symbols, and

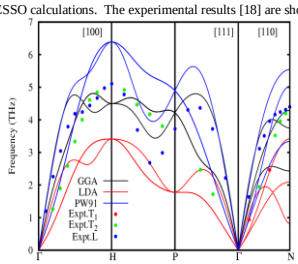

Fig 4: Tantalum dispersion curves. GGA(PBE), LDA and PW91 results. The experimental results from the inelastic neutron scattering data [19]are shown by the symbols, and

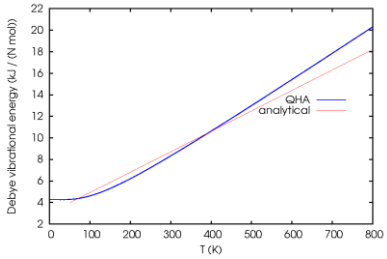

Fig 5: The internal energies ΔE of Molybdenum. Analytical (IFCs) calculated values in the pink line; First principle (QUANTUM ESPRESSO) calculated values in blue line

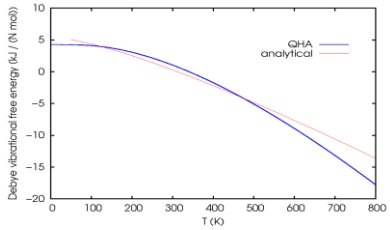

Fig 6: The Helmholtz free energies ΔF of Molybdenum. Analytical (IFCs) calculated values in the pink line; First principle calculated values in blue line

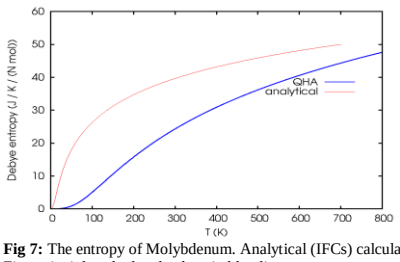

Fig 7: The entropy of Molybdenum. Analytical (IFCs) calculated values in the pink line; First principle calculated values in blue line

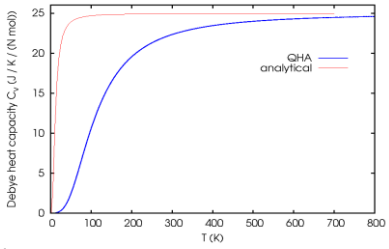

Fig 8: The C_v for Molybdenum. Analytical (IFCs) in the pink line dispersion; First principle calculated values in blue line

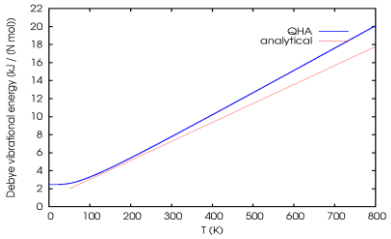

Fig 9: The phonon contribution to the internal energies ΔE of Tantalum. Analytical (IFCs) calculated values in the pink line; First principle calculated values in blue line

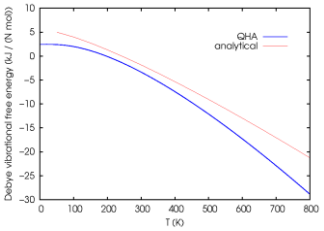

Fig 10: The phonon contribution to the Helmholtz free energies ΔF of Tantalum. Analytical (IFCs) calculated values in the pink line; First principle calculated values in blue line

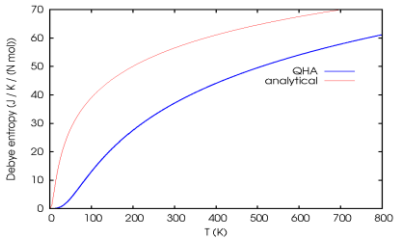

Fig 11: The entropy of Tantalum. Analytical (IFCs) calculated values in the pink line; First principle calculated values in blue line

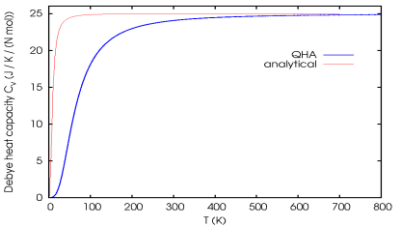

Fig 12: The C_v for Tantalum. Analytical (IFCs) in pink line; First principle calculated values in blue line

Table 1: (a) Frequencies and calculated percentage errors at some high symmetry points for Molybdenum (Mo). (b Calculated MAE and MARE for Molybdenum.

	a_T	FREQUENCY (THz)						
	$(a.u)$	H_L	H_T	P_L	P_T	N_L	N_{T_1}	N_{T_2}
GGA(PAW)	5.99	6.6726	6.6726	6.1009	6.1009	7.5130	4.4645	5.3168
PW91	6.02	5.9781	5.9781	6.6026	6.6026	8.0528	4.4545	5.8246
LDA	5.91	6.6602	6.6602	6.0387	6.0387	7.6225	4.3982	5.1306
IFCs	-	6.3554	6.3554	6.6734	6.6734	8.0225	4.9257	5.7529
Expt. [a]	5.947	6.4395	5.6369	6.5032	6.5096	8.2229	4.6051	5.7643
				% Error				
GGA(PAW)	0.72	3.62	18.37	6.17	6.28	8.63	3.05	7.76
PW91	1.23	7.17	6.05	1.53	1.43	2.07	3.27	1.05
LDA	-0.62	3.43	18.15	7.14	7.23	7.30	4.49	10.99
IFCs	-	1.31	12.74	2.62	2.52	2.44	6.96	0.20

(a)

	TOTAL	AVERAGE	$\pm(work - expt.)$ **(THz)**	MAE(THz)	MARE (%)
GGA(PAW)	42.8413	6.1202	0.8402	0.1200	1.92
PW91	43.4933	6.2133	0.1882	0.0269	0.43
LDA	42.5491	6.0784	1.1324	0.1618	2.59
IFCs	44.7587	6.3941	1.0772	0.1539	2.47
Expt. [a]	43.6815	6.2402	-	-	-

(b)

[a][18] (Experiment)

Table 2: (a) Frequencies and calculated percentage errors at some high symmetry points for Tantalum (Ta). (b) Calculated MAE and MARE for Tantalum.

	a_T	FREQUENCY (THz)						
	$(a.u)$	H_L	H_T	P_L	P_T	N_L	N_{T_1}	N_{T_2}
GGA(PBE)	6.28	4.4978	4.4978	4.2166	4.2166	4.2908	2.4299	3.7510
PW91	6.27	6.3895	6.3895	4.8935	4.8935	5.5420	3.3389	5.0255
LDA	6.14	3.4133	3.4133	1.7771	1.7771	3.4189	0.8153	2.0944
IFCs		5.0662	5.0662	3.6928	3.6928	4.3486	2.5274	4.3000
Expt. [b]	6.239	5.1073	4.9158	3.7215	3.8071	4.3981	2.4620	4.1943
				% Error				
GGA(PBE)	0.66	11.93	8.50	13.30	10.76	2.44	1.30	10.57
PW91	0.50	25.11	29.98	31.49	28.54	20.64	35.62	19.82
LDA	-1.59	33.17	30.56	52.25	53.32	22.26	66.88	50.07
IFCs	-	0.80	3.06	0.77	3.00	1.13	2.66	2.52

(a)

	TOTAL	AVERAGE	$\pm(work - expt.)$ **(THz)**	MAE(THz)	MARE (%)
GGA(PBE)	27.9005	3.9858	0.7056	0.1008	2.66
PW91	36.4724	5.2103	7.8663	1.1238	27.50
LDA	16.7094	2.3871	11.8967	1.6995	41.59
IFCs	28.6940	4.0991	0.0879	0.0126	0.31
Expt. [b]	28.6061	4.0866	-	-	-

(b)

[b] [19] (Experiment).

4 CONCLUSION

The dispersion curves and thermodynamic properties of Mo and Ta were calculated successfully using two techniques; the interatomic force constants (IFCs) technique employing the Born – von Kármán model and the first principle technique based on DFT implemented by QUANTUM ESPRESSO. The phonon dispersions were computed along the principal symmetry points of the BZ. The results obtained from both techniques were matched with data from experiment. We conclude that the phonon dispersion curve of Mo from first principle calculation is in better agreement with experiment compared to the IFCs calculation, whereas, the phonon dispersion curve of Ta from IFCs is in better agreement with experiment compared to the first principle calculation.

REFERENCES

[1] Da Cunha Lima, I. C., Brescansin, L. M and Shukla, M. M. (1974). Lattice Dynamics of Alkali Metals. *Physica* 72, 179 – 187.

[2] Baroni, S., de Gironcoli, S., Dal Corso, A. and Giannozzi. P. (2001). Phonons and related crystal properties from density-functional perturbation theory. *Rev. Mod. Phys*., **73**:515

[3] Hohenberg, P. and Kohn, W. (1964). Inhomogeneous electron gas. *Phys. Rev*. B 136, 864

[4] Kohn, W. and Sham, L. J. (1965). Self-consistent equations including exchange and correlation effects. *Phys. Rev*. 140, A1133

[5] Zein, E. N. (1984). Density Functional Calculations of Elastic Moduli and Phonon Spectra of Crystals. *Fiz. Tverd. Tela* (Leningrad) **26** 3024 *Sov. Phys. Solid State***26**, 1825

[6] Baroni, S., Giannozzi, P. and Testa, A. (1987). Green's-function approach to linear response in solids. *Phys. Rev. Lett*. 58, 1861

[7] Jones, R. O. and Gunnarson, O. (1989). The density functional formalism, its applications and prospects. *Rev. Mod. Phys*. 61, 689.

[8] Becke, A. D., (1988). Density-functional exchange-energy approximation with correct asymptotic behavior. *Phys. Rev*. A 38, 3098.

[9] Perdew, J. P., Burke, K. and Ernzerhof, M. (1996). Generalized gradient approximation made simple. *Phys. Rev. Lett*. **77**, 3865.

[10] Dal Corso, A. (2013). Ab-initio phonon dispersions of transition and noble metal: effects of the exchange and correlation functional. *J. Phys.: Condensed Matter*, 25, 1-9

[11] Giannozzi, P., Baroni, S., Bonini, N., Calandra, M., Car, R., Cavazzoni, C., Ceresoli, D., Chiarotti, G. L., Cococcioni, M., Dabo, I., Dal Corso, A., Fabris, S., Fratesi, G., de Gironcoli, S., Gebauer, R., Gerstmann, U., Gougoussis, C., Kokalj, A., Lazzeri, M., Martin-Samos, L., Marzari, N., Mauri, F., Mazzarello, R., Paolini, S., Pasquarello, A., Paulatto, L., Sbraccia, C., Scandolo, S., Sclauzero, G., Seitsonen, A. P., Smogunov, A., Umari, P. and Wentzcovitch, R. M. (2009). QUANTUM ESPRESSO: a modular and open-source software project for quantum simulations of materials. *J. Phys.: Condens. Matter***21**, 395502.

[12] Giannozzi, P., Andreussi, O., Brumme, T, Bunau, O., Nardelli, M. B., Calandra, M., Car, R., Cavazzoni, C., Ceresoli, D., Cococcioni, M., Colonna, N., Carnimeo, I., Dal Corso, A., de Gironcoli, S., Delugas, P., DiStasio Jr, R. A., Ferretti, A., Floris, A., Fratesi, G., Fugallo, G., Gebauer, R., Gerstmann, U., Giustino, F., Gorni, T., Jia, J., Kawamura, M., Ko, H-Y., Kokalj, A ., Küçükbenli, E., Lazzeri, M., Marsili, M., Marzari, N., Mauri, F., Nguyen, N. L., Nguyen, H-V., Otero-de-la-Roza, A., Paulatto, L., Poncé, S., Rocca, D., Sabatini, R., Santra, B., Schlipf, M ., Seitsonen, A. P., Smogunov, A., Timrov, I., Thonhauser, T., Umari, P., Vast, N., Wu, X., and Baroni, S. (2017). Advanced capabilities for materials modelling with Quantum ESPRESSO. *J. Phys.: Condensed. Matter.* Vol. 29. **24.**

[13] Gilat, G. and Raubenheimer, L. T. (1966). Accurate numerical method for calculating frequency-distribution functions in solids. *Phys. Rev*. 144, 390

[14] Landau, L. D. and Lifshitz, E. M. (1980). *Statistical Physics*, 3rd. ed. (Pergamon, London), Pt. 1, Pp. 193.

[15] Changyol, L. and Xavier, G. (1995). Ab-initio calculation of the thermodynamic properties and atomic temperature factors of SiO_2 α-quartz and stishovite. *Phys. Rev*. B 51, 8610.

[16] Peng, F.,ZhiFu, H., and LuCheng, X. (2007). First-principles calculations of thermodynamic properties of TiB_2 at high pressure. *Physica B: Condensed Matter*. Vol. 400, Issues 1–2, Pg. 83-87.

[17] Minamoto, S., Kato, M.,Konashi, K., and Yoshiyuki Kawazoe, Y. (2009). Calculations of thermodynamic properties of PuO_2 by the first-principles and lattice vibration. *Journal of Nuclear Materials*. Vol. 385, Issue 1, Pg. 18-20

[18] Woods, A. D. B., Chen S. H., (1964). Lattice dynamics of Molybdenum. *Solid State Comm.* 2, Pp 233-237.

[19] Woods, A. D. B. (1964). Lattice dynamics of Tantalum. *Phys. Rev*. **136**, 3A, pp A781- A783